Conditioned Medium of Bone Marrow Mesenchymal Stem Cells Relieves Acute Lung Injury in Mice by Regulating Epithelial Sodium Channels via miR-34c

Zhiyu Zhou
China Medical University
Yong Cui
China Medical University First Hospital
Yapeng Hou
China Medical University
Tong Yu
China Medical University
Yan Ding
China Medical University
Hongguang Nie (hgnie@cmu.edu.cn)
China Medical University https://orcid.org/0000-0002-9973-6354

Research

Keywords: mesenchymal stem cells, conditioned medium, acute lung injury, epithelial sodium channels, miR-34c

Posted Date: September 3rd, 2020

DOI: https://doi.org/10.21203/rs.3.rs-67843/v1

Conditioned medium of bone marrow mesenchymal stem cells relieves acute lung injury in mice by regulating epithelial sodium channels *via* miR-34c

Zhiyu Zhou,[1] Yong Cui,[2] Yapeng Hou,[1] Tong Yu,[1] Yan Ding,[1] and Hongguang Nie[1*]

[1]*Department of Stem Cells and Regenerative Medicine, College of Basic Medical Science, China Medical University, Shenyang, 110122, China*

[2]*Department of Anesthesiology, the First Affiliated Hospital of China Medical University, Shenyang, 110001, China*

*Correspondence: hgnie@cmu.edu.cn

Abstract

Aims: One of the characteristics of acute lung injury (ALI) is severe pulmonary edema, which is closely related to alveolar fluid clearance. Mesenchymal stem cells (MSCs) secrete a wide range of cytokines, growth factors and miRNAs through paracrine action to participate in the mechanism of pulmonary inflammatory response, which increases the clearance of edema fluid, and promotes the repair process of ALI. However, the mechanism by which bone marrow derived MSCs-conditioned medium (BMSCs-CM) promotes edema clearance is unclear. Epithelial sodium channel (ENaC) is the rate-limiting step in the sodium-water transport and edema clearance in the alveolar cavity, and we aim to explore the role of ENaC in BMSCs-CM invloved edema clearance and whether it can alter the function of ENaC *via* miRNAs.

Methods: CCK-8 cell proliferation assay was used to detect the effect of BMSCs-CM on the survival of AT2 cells. Real-time PCR (RT-PCR) and Western blot were used to detect the expression of ENaC in AT2 cells. The effects of exosomes/miR-34c on the transepithelial short-circuit current in the monolayer of H441 cells were examined by the Ussing chamber setup. Dual luciferase reporter gene assay was used to detect the target gene of miR-34c.

Results: BMSCs-CM can increase the viability of mouse AT2 cells. RT-PCR and Western blotting results showed that BMSCs-CM significantly increased the expression of γ-ENaC subunit in mouse AT2 cells. Ussing chamber assay revealed that BMSCs-CM enhanced the amiloride-sensitive currents associated with ENaC activity in intact H441 cell monolayers. In addition, we observed higher expression of miR-34c in mouse AT2 cells administrated with BMSCs-CM, and the overexpression or inhibition of miR-34c can regulate the expression of ENaC protein and alter the function of ENaC. Finally, we detected MARCKS may be one of the target gene of miR-34c.

Conclusions: Our results indicate that BMSCs-CM may improve LPS-induced ALI through miR-34c targeting MARCKS and regulating ENaC indirectly, which further explores the benefit of paracrine effects of BMSCs on edematous ALI.

Keywords: mesenchymal stem cells, conditioned medium, acute lung injury, epithelial sodium channels, miR-34c

Introduction

Acute lung injury (ALI), a common clinical complication, is caused by various intrapulmonary and extrapulmonary factors other than cardiogenic. Alveolar fluid clearance (AFC) is closely related to pulmonary edema, one of the characteristics of ALI [1, 2]. When AFC is enhanced, the removal of alveolar accumulation fluid is accelerated, which contributes to the relief of pulmonary edema [3]. In the lung, epithelial sodium channel (ENaC) is the rate-limiting step in the AFC process, and the primary way to complete the sodium-water transport in alveolar type 2 epithelial (AT2) cells and edema clearance in the alveolar cavity [4-6]. Decreased expression of ENaC will lead to the formation of edema, emphasize that regulation of ENaC is essential for pulmonary edema clearance in patients with edematous ALI [7].

Mesenchymal stem cells (MSCs) are non-hematopoietic adult stem cells with strong self-renewal ability while maintaining their pluripotency [8, 9]. They can differentiate into a variety of cells under specific induction conditions *in vivo* or *in vitro*, and thus can be used to repair damaged and diseased multiple tissues and organs [10, 11]. Moreover, they have the advantages including easy isolation and better reproductive ability *in vitro*, and have the characteristics of low immunogenicity, reduced immune rejection [12, 13]. In addition, their application does not involve the ethical problems [12, 14]. Therefore, they are widely used in the treatment of various lung diseases in clinical practice, such as ALI, chronic obstructive pulmonary disease, asthma and pulmonary fibrosis.

MSCs release multiple microRNAs (miRNAs) into conditioned medium, which may involve in the benefits of MSCs in re-alveolarization during MSC-induced reparative processes of injured respiratory epithelium in injured lungs [15]. This feature can regulate the permeability of endothelium and epithelium, participate in inflammatory response, increase AFC, repair tissue damage, and exert various biological functions [16, 17]. MiRNAs, small non-coding RNAs, belong to single-stranded RNA segments with approximately 20-24 nucleotides in length. They are involved in the transcriptional and post-transcriptional modification of protein-coding gene expression [18]. The translation process of the mRNA molecule is

inhibited by complete or incomplete pairing with the complementary sequences of 3'-UTR of targeting mRNAs [19]. Apparently, miRNAs negatively alter the synthesis of the corresponding proteins and ultimately regulate multiple cellular activities [20, 21]. The levels of miRNA expression change according to cell stressors, which may play a critical role in the progression and maintenance of lung diseases [22].

Direct administration of MSCs has been shown to be effective in clinical trials which is definitively the case here, but if the beneficial effects of MSCs-conditioned medium (MSCs-CM) are as good as those seen with cell-based therapy, this therapeutic strategy would be simpler and with fewer potential limitations [23]. Lots of studies have reported the effects of bone marrow derived MSCs (BMSCs) on ALI [26,27], but there has rarely been reported that BMSCs-CM reliefs edematous ALI by regulating alveolar epithelial ion transport. In this research, we researched BMSCs-CM in exploring cell-free therapy and identified that miRNAs released by BMSCs-CM could regulate ENaC to improve edema clearance, which may be considered as the interesting targets for treating edematous lung diseases development and providing a new pharmacological strategy as well [28].

Materials and Methods

Animals

Pathogen-free C57 mice were purchased from Liaoning Changsheng Biotechnology Co., Ltd., and the animal certificate number is SCXK (Liao) 2018-0001. All experimental methods involving C57 mice were performed in accordance with the guidelines of the Animal Care and Use Ethics Committee (Certificate Number: CMU2019088), and all protocols were approved by China Medical University.

Isolation, culture and identification of mouse BMSCs and AT2 cells

Three-week-old pathogen-free male C57 mice weighing 9-13 g were anaesthetized by diazepam (17.5 mg kg^{-1}, intraperitoneally) followed 6 min later by ketamine (450 mg kg^{-1}, intraperitoneally). The femora were isolated. Bone marrow was collected by gently washing medullary cavity of femora with DMEM/F12

medium (HyClone) supplemented with 10% fetal bovine serum (FBS, Gibco), 10 ng/ml recombinant mouse basic fibroblast growth factor (PeproTech), 100 IU penicillin, and 100 μg/ml streptomycin. Then it was cultured in humidified incubator (5% CO_2, 37ºC) for 24 h. The medium was first changed to remove non-adherent cells and tissues, then replaced every other day. At 80% confluence, the medium of BMSCs was changed and replaced by FBS-deprived DMEM/F12 medium. BMSCs-CM was collected in 24 h and stored at -80ºC freezer post filtering with 0.22 μm filter. The cells were incubated with the antibody (FITC-labeled CD34 or APC-labeled CD44) at 37°C for 30 min for identification, and detected by flow cytometry.

Lung stripping of newborn C57 mice (within 24 h) was placed in pre-chilled PBS and then minced, digested with 0.25% trypsin and 0.1% type I collagenase at 37°C for 30 min, respectively. Cells were filtrated and cultured in 5% CO_2, 37ºC atmosphere in DMEM/F12 containing 10% FBS (Gibco), 100 IU penicillin and 100 μg/ml streptomycin for 45 min. Unattached cells were collected and repeated the above culture process for 4 times to remove lung fibroblast cells. Then the cell suspension was transferred on IgG coated culture dish and incubated for 30 min to remove lymphocytes, macrophages, and neutrophils. Unattached cells were adjusted to 2-3 × 10^6/mL and the medium was changed after 72 h for the first time, then changed every other day. For identification of AT2 cells, the cells were fixed with 4% paraformaldehyde for 30 min, and SP-C antibody was added to the slide and placed in a wet box at 4°C overnight. The next day FITC fluorescently labeled secondary antibody was added to the slide, which was placed in a wet box for 1 h at 37°C in the dark. The cells were counterstained with 5 mg/L DAPI for 10 min, washed and observed with a fluorescence microscope.

CCK-8 cell proliferation assay

Primary mouse AT2 cells were seeded in 24-well plates and cultured in DMEM/F12 medium containing 10% FBS in a 5% CO_2, 37°C cell incubator for 12 h. Thereafter, the medium containing 10% CCK-8 was added and the cells were incubated for 1 h in the dark. The initial OD (0 point) value was measured at 450

nm using a microplate reader. The cells in the 24-well plate were randomly divided into 4 groups: the first group was cultured in normal DMEM/F12 medium containing 10% FBS (control group, Control), the second group was cultured in serum-free DMEM/F12 medium (serum-free group, SD), the third group was co-cultured with BMSCs (co-culture group, Co-culture), and the fourth group was administrated with BMSCs-CM (conditioned medium group, CM). After 24 h, the original medium was aspirated, and DMEM/F12 medium containing 10% CCK-8 was added to measure the OD value and calculate the cell survival rate accordingly.

Ussing chamber assay

Human distal lung epithelial cell line NCI-H441 was obtained from the American Type Culture Collection (ATCC) and cultured as previously described. H441 cells were grown in RPMI medium (ATCC) containing 10% FBS, 2 mM L-glutamine, 10 mM HEPES, 1 mM sodium pyruvate, 4.5 g/L glucose, 1.5 g/L sodium bicarbonate and antibiotics (100 U/ml penicillin and 100 μg/ml streptomycin). For Ussing chamber assays, cells were seeded on permeable support filters (Costar) at a supraconfluent density (~5×10^6 cells/cm^2), and incubated in a humidified atmosphere of 5% CO_2 at 37°C. Dexamethasone (250 nM, Sigma) was supplemented to stimulate ENaC expression. Cells reached confluency in the Costar Transwells 24 h after plating. At this point media and non-adherent cells in the apical compartment were removed to adapt the cells to air-liquid interface culture. Culture media in the basolateral compartment was replaced every other day, whereas the apical surface was rinsed with PBS. Transepithelial resistance was measured by an epithelial tissue volt-ohm-meter (World Precision Instruments). Highly polarized tight monolayers with resistance > 500 Ω cm^2 were used for measuring short-circuit current (Isc) levels of transepithlium.

Measurements of transepithelial Isc and resistance were performed as described previously in H441 monolayers. In brief, H441 monolayers were mounted in Ussing chambers (Physiologic Instrument) and then bathed on both sides with a solution containing (in mM): 120 NaCl, 25 $NaHCO_3$, 3.3 KH_2PO_4, 0.83 K_2HPO_4, 1.2 $CaCl_2$, 1.2 $MgCl_2$, 10 HEPES sodium salt and either 10 mannitol for apical compartment or 10

D-glucose for basolateral compartment. The pH of each solution was adjusted to 7.4 and the osmolality was 290-300 mOsm/kg. The solutions of both sides were bubbled with mixed gas containing 95% O_2 and 5% CO_2 at 37ºC. Isc was measured with Ag-AgCl electrodes filled with 4% agar in 3 M KCl. The monolayers were short-circuited to 0 mV, and a 10 mV pulse of 1s was applied every 10 s to monitor the resistance of transepithelium. Acquire and Analyze 2.3 program was used to collect data. ENaC activity is the reduction of Isc after adding amiloride to the apical side (100 μM).

Western blot assay

H441 and mouse AT2 cells were cultured in 6-well plates, washed with PBS when cells were fused to 80%, and then assayed by immunoblotting. Proteins were separated on 10% SDS-PAGE gels and transferred to PVDF membranes (Invitrogen). The blots were incubated in blocking solution containing 20 mM Tris-HCl (pH 7.5), 0.5 M NaCl, 1% Tween (TBST) and 5% BSA for 1 h at room temperature. Membranes were incubated with 1:2000 in TBST with 5% BSA of γ-ENaC antibody (Thermo Fisher) or β-actin (Santa Cruz Biotechnology) overnight at 4°C. Following washing three times with TBST, membranes were incubated with HRP conjugated goat-anti-rabbit or goat-anti-mouse secondary antibody at 1:2000 at room temperature for 1 h and then washed for 10 min with TBST for three times. Images were developed by an enhanced ECL kit and collected by the Image J program.

Real-time polymerase chain reaction

Total RNA was extracted using TRIzol reagent (Invitrogen) according to the manufacture instructions. Spectrophotometry was used to measure the concentration and purity of total RNA. Reverse transcription was performed using a PrimeScript RT reagent Kit with gDNA Eraser (TaKaRa). Real-time polymerase chain reaction (RT-PCR) with SYBR Premix Ex Taq II (TaKaRa) was performed using ABI7500. GAPDH was used as a reference. The following primer pairs were used: γ-ENaC, 5′-GCACCG TTC GCC ACC TTC TA-3′ (sense), 5′-AGG TCA CCA GCA GCT CCT CA-3′ (antisense); GAPDH, 5’-AGA AGG CTG GGG CTC ATT TG-3’ (sense), 5’-AGG GGC CAT CCA CAG TCT TC-3’ (antisense). miR-34c, 5’-AGG CAG

UGU AGU UAG CUG AUU GC-3' (sense), 5'-AAU CAG CUA ACU ACA CUG CCU UU-3' (antisense). The expression levels of miR-34c were measured using the Mir-X miRNA First-Strand Synthesis Kit (TaKaRa). U6 was used as a reference. The final volume is 15 μl. The reaction conditions of the miRNA were a single cycle of 95°C for 30 s, 5 s at 95 ° C, and 40 cycles at 60 ° C for 30 s. The data from RT-PCR were analyzed using the $2^{-\triangle\triangle CT}$ method.

Transfections

H441 and AT2 cells were cultured in a six-well plate. When the cells were fused to 50-60%, the serum-containing medium was discarded, and then the cells were replaced with serum-free medium after washing with PBS. Negative control, miR-34c mimics, inhibitor negative control, or miR-34c inhibitor (GenePharma) was transfected into cells with siRNA-mate (GenePharma) according to the manufacturer's instructions, respectively. The final concentration of miR-34c mimics was 30 nM and miR-34c inhibitor was 60 nM. All transfection reagents were removed after 6 h and cells were used 48 h post transfection.

Dual luciferase reporter gene assay

The dual luciferase reporter gene detects the regulation of genes by reflecting the amount of luciferase expression. It detects the fluorescence intensity of fluorescein substrate after transfecting cells with a reporter plasmid. H441 cells were cultured in a six-well plate, and fused to 60-70%. The serum-containing medium was discarded, and the cells were replaced with serum-free medium. The constructed MARCKS-3'UTR wild-type and mutant recombinant plasmids (GenePharma) were transfected into H441 cells with miR-34c mimics or negative control, respectively. After 48 h, luciferase activity was measured using the Dual Luciferase Reporter Assay Kit (Vazyme), according to the manufacturer's instructions.

Statistical analysis

Data were expressed as the mean ± SE. ENaC activity is the difference of the total and amiloride-resistant current fractions. Normality and homoscedasticity test was done by Levene and Shapiro-Wilk test before applying parametric tests. For comparison of two groups, we used Student's two-tailed t-test; for comparison

of multiple groups, we performed one-way analyze of variance (ANOVA) followed by Bonferroni's test for all the groups of the experiment. When the data did not pass the normality or homoscedasticity test, we used a non-parametric t-test (Mann-Whitney U-test). Variations were considered significant when the *P*-value was less than 0.05. Statistical analysis was performed with Origin 8.0.

Results

Identification of BMSCs and AT2 cells

As shown in Supplementary Fig. 1 (A, B), the second generation mouse BMSCs were trypsinized and counted. After 1×10^6 cells were incubated with antibodies as CD34 and CD44, BMSCs were identified by flow cytometry. The CD44 positive expression rate was 92.5%, whereas CD34 negative expression rate was 97.3%. Supplementary Fig. 2 (A-C) is the immunofluorescence result of AT2 cells stained with DAPI, SP-C or both, respectively.

BMSCs and BMSCs-CM enhance the viability of mouse AT2 and H441 cells

To investigate the effect of BMSCs on the cell viability by CCK-8 cell proliferation assay, we first co-cultured BMSCs with primary mouse AT2 and H441 cells, respectively. As shown in Fig. 1A, co-culture of BMSCs and primary AT2 cells significantly improved cell survival, compared with the serum-free (SD) group ($P < 0.01$, n = 6). Meanwhile, administration of BMSCs-CM also increased viability of AT2 cells ($P < 0.01$, n = 6, compared with SD group). As expected, BMSCs and BMSCs-CM were also able to increase the survival rate in H441 cells ($P < 0.01$, n = 5, compared with the SD group, Fig. 1B). Accordingly, both BMSCs and BMSCs-CM can enhance the viability of mouse AT2 and H441 cells, and we administrated BMSCs-CM in the following experiments.

BMSCs-CM increases the protein and mRNA expression of γ-ENaC in mouse AT2 and H441 cells

We further examined the effects of BMSCs-CM on ENaC at the protein expression levels in mouse AT2 and

H441 cells, respectively. As shown in Fig. 2A-B, a specific band of γ-ENaC between 70 and 100 kD was observed by western blot assay according to the manufacturer's manual. LPS downregulated γ-ENaC expression in AT2 cells compared with Control group ($P < 0.01$), and BMSCs-CM increased the protein expression of γ-ENaC in both primary and LPS-treated AT2 cells ($P < 0.01$ compared with Control and LPS group, respectively, n = 5). Similar results were observed in H441 cells and LPS-induced ALI cell model ($P < 0.01$ compared with Control and LPS group, respectively, n = 7). We speculate the higher protein expression of γ-ENaC was associated with the increased transcription level, which was confirmed by the RT-PCR results that incubating with BMSCs-CM caused a significant increase of γ-ENaC mRNA expression in primary and LPS-treated AT2 cells ($P < 0.05$ and $P < 0.01$ compared with Control and LPS group, respectively, n = 5, Fig. 2C).

BMSCs-CM enhances the expression of miR-34 in mouse AT2 cells

Previous studies suggested that miR-34c involved in the corresponding pathways related to LPS-induced ALI [24]. In our experiment, we analyzed the expression levels of miR-34c in mouse AT2 cells after BMSCs-CM administration. As shown in Fig. 3A, we found that exposure to LPS caused a significant decrease in miR-34c level compared with Control group ($P < 0.01$). Conversely, the levels of miR-34 increased in normal and LPS-treated mouse AT2 cells after administration of BMSCs-CM ($P < 0.05$ and $P < 0.01$ compared with Control and LPS group, n = 6), respectively. These data proved that the expression level of miR-34c decreased during ALI and BMSCs-CM upregulated the level of miR-34c in LPS-induced ALI cell model.

The level of miR-34c is positively correlated with γ-ENaC in mouse AT2 cells

Based on the above facts that BMSCs-CM could both upregulate the expression levels of γ-ENaC and miR-34c, we assume that BMSCs-CM may enhance the expression of γ-ENaC protein through miR-34c accordingly. To test this hypothesis, mouse AT2 cells were transfected with miR-34c mimics (Mimic) or inhibitor (Inhibitor), respectively. Transfection efficiency of miR-34c was verified by RT-PCR (n = 4, Fig.

3B). The effect of miR-34c on γ-ENaC was examined by western blot analysis, and the histogram was illustrated for the sake of comparison (Fig. 4). Transfection of miR-34c mimics into mouse AT2 cells resulted in a significant increase of γ-ENaC expression compared with negative control (NC) group ($P < 0.05$), while inhibition of miR-34c showed opposite effects ($P < 0.01$, n = 3). These data suggested that miR-34c increased the protein expression of γ-ENaC. The potential mechanism of BMSCs-CM protection in ALI may be related to the enhanced miR-34c level and sequent stimulation of γ-ENaC protein expression.

MiR-34c increases transepithelial short-circuit current in confluent H441 monolayers

Human bronchoalveolar epithelial-derived Clara (H441) cells have been widely used to study the function of ENaC in the lung, and the ENaC characteristics of H441 are similar to those of primary AT2 cells, which could hardly grow into monolayers [4, 25]. In our recent study, BMSCs-CM has been proved to activate amiloride-sensitive Isc (ASI), which reflects ENaC activity in LPS-treated H441 monolayers [26]. In order to further confirm the functional regulation of ENaC by miR-34c, we measured Isc in confluent H441 monolayers. As shown in Fig. 5, ASI was defined as the difference between the total current and the amiloride-resistant current, and the negative control (NC) was set as 100%. MiR-34 significantly increased the ASI of H441 monolayers to 132.3 ± 8.4% ($P < 0.01$, compared with NC, n = 5), which indicates that miR-34c could enhance the fluid transport of lung through increasing ENaC activity in alveolar epithelial cells.

MiR-34c may upregulate ENaC expression by binding to the 3'-UTR of MARCKS

Potential miR-34c targets were predicted using in silico approaches and according to the bioinformatic website prediction, we postulate that myristoylated alanine-rich C kinase substrate (MARCKS), a nagative regulator of ENaC, might be a potential target of miR-34c [27, 28]. To confirm this finding, a dual luciferase target gene assay was conducted. Wild-type (WT) and mutant reporter gene vectors (MT) for MARCKS were constructed and as shown in Fig. 6, mouse AT2 cells were co-transfected with the vectors (NC) and miR-34c mimics (Mimic). After 24 h, the *firefly* luciferase activity was measured. *Firefly* luciferase units

were normalized with *Renilla* luciferase units. We found that the expression of pmirGLO-MARCKS-WT (Mimic + WT) relative luciferase activity was reduced significantly by miR-34c ($P < 0.01$, compared with NC + WT), while the expression of pmirGLO-MARCKS-MT (Mimic + MT) was not suppressed by miR-34c ($P > 0.05$, compared with NC + MT, n = 5). The above data verified that MARCKS is one of the target genes of miR-34c, which could upregulate ENaC expression by binding to the 3'-UTR of MARCKS.

Discussion

MSCs are being extensively investigated for their potential in tissue engineering and regenerative medicine [29]. Of note, BMSCs have many advantages, such as extensive sources, easy to culture *in vitro*, and less ethical issues, so the study of BMSCs is more extensive at present. Researchers have reported that MSCs can exert beneficial effects by their released extracellular vesicles, however, whether ENaC is involved in the above process is still rarely known [30]. It has been confirmed that patients with ALI have disorders of pulmonary fluid clearance, and evidence has also shown that reabsorption of Na^+ by ENaC is an important step to maintain the balance of alveolar fluid [31].

In our experiment, we first used CCK-8 cell proliferation assay to prove the influence of BMSCs-CM on the viability of alveolar epithelial cells, which can increase the survival rate of both mouse AT2 and H441 cells. In order to verify whether BMSCs-CM can regulate ENaC, we next studied the effect of BMSCs-CM on ENaC expression in mouse AT2 cells. The stimulation of α-ENaC in AT2 cells has been proved in our recent study, we future identified the similar enhancement of γ-ENaC expression by BMSCs-CM at protein and mRNA levels [26].

The miRNAs are short (approximately 22 nucleotides) and noncoding RNAs, which function as post-transcriptional repressors of gene expression by binding predominantly to the 3'-UTR of mRNAs to interfere with protein production [32, 33]. The involvement of miRs in ALI is still seldom known [34]. We tried TargetScan and Miranda software for the prediction, while using DIANA-microT to screen the

identical miRNAs. Finally we chose miR-34c for the Na^+ regulation in our study, which has been identified to be related with LPS-induced ALI [24]. Based on the upregulation of γ-ENaC and possibly beneficial effects of BMSCs-CM in ALI, we speculate that the miRNAs secreted by BMSCs to the medium, especially miR-34c might be involved. The expression of miR-34c decreased in LPS group whereas increased significantly in BMSCs-CM group, indicating that miR-34c might participate in the ENaC regulation of BMSCs-CM in alveolar epithelial cells.

The evidence that BMSCs-CM can increase the protein and mRNA expression of ENaC and the higher expression of miR-34c in BMSCs-CM, makes us suppose that miR-34c might also stimulate the expression of ENaC. Then we transfected miR-34c mimics or inhibitor into mouse AT2 cells, respectively. As expected, western blot analysis showed that miR-34c could significantly increase the protein expression of γ-ENaC, while the inhibitor of miR-34c exhibited the opposite effects. The human lung adenocarcinoma cell line H441 is one of the classical cell lines for studying the function and activity of ENaC. In our previous studies, Ussing chamber assay was used to record the Isc in confluent H441 monolayers [4]. To test the effects of miR-34c on ion channel function, we calculated the ASI which reflected ENaC activity, and revealed that miR-34c could increase ASI in intact H441 monolayers.

From above, we can see that BMSCs-CM could protect edematous lung injury by increasing the protein and mRNA expression of γ-ENaC, which may be related with miR-34c. Then a question arose, how miR-34c regulates γ-ENaC? The negative control of miRNAs and their target genes almost excluded the direct binding of miR-34c with ENaC, and we investigated the possible regulator-MARCKS, which is both an upstream factor of ENaC and a possible effector of miR-34c. The double luciferase reporter gene identified the direct binding of miR-34c with MARCKS, whereas MARCKS phosphorylation was found to decrease ASI in a time- and dose-dependent manner and ENaC activity could also be regulated by calpain-2 proteolysis of MARCKS proteins [28, 35]. Our results showed that miR-34c can act on γ-ENaC indirectly, and MARCKS might be one of its target genes, through which miR-34c inhibits the expression and activity

of γ-ENaC (Fig. 7). This topic studied the possible mechanisms of BMSCs-CM in the treatment of LPS induced ALI at the molecular level, which would provide a theoretical basis and therapy target for ALI related edematous lung diseases.

Conclusions

BMSCs-CM can increase LPS-induced ENaC expression and function in ALI at least by upregulating miR-34c, and MARCKS is one of its target genes. These findings will further explore the therapeutic effects of paracrine effects of BMSCs on edematous lung diseases.

Abbreviations

ALI: Acute lung injury; AFC: Alveolar fluid clearance; ENaC: Epithelial sodium channel; miRNA: microRNA; MSCs: Mesenchymal stem cells; MSCs-CM: MSCs-conditioned medium; AT2 cells: Alveolar type 2 epithelial cells; FBS: Fetal bovine serum; LPS: Lipopolysaccharide; RT-PCR: Real-time polymerase chain reaction; Isc: Short-circuit current.

Acknowledgements

Not applicable.

Authors' contributions

H.N conceived and designed the study. Z.Z, Y.C, Y.H and Y.D performed the study. Z.Z and T.Y analyzed the data. Z.Z and H.N drafted the manuscript. Y.C revised the draft of manuscript. All authors corrected and approved the final version of the manuscript.

Funding

This work was supported by grants from the National Natural Science Foundation of China (NSFC 81670010), Provincial Key Research and Development Program Guidance Project (2018225077), and Basic Research Project of Liaoning Higher School (LQNK201745).

Availability of data and materials

The datasets used and analysed during the current study are available from the corresponding author on reasonable request.

Ethics approval and consent to participate

This study followed the national guidelines and protocols of the National Institutes of Health and was approved by the Local Ethics Committee for the Care and Use of Laboratory Animals of China Medical University.

Competing interests

All authors declare that they have no competing interests.

References

1. Jiang L, Fei D, Gong R, Yang W, Yu W, Pan S, et al. CORM-2 inhibits TXNIP/NLRP3 inflammasome pathway in LPS-induced acute lung injury. Inflamm Res. 2016;65(11):905-15.
2. Zhang S, Danchuk SD, Bonvillain RW, Xu B, Scruggs BA, Strong AL, et al. Interleukin 6 mediates the therapeutic effects of adipose-derived stromal/stem cells in lipopolysaccharide-induced acute lung injury. Stem cells (Dayton, Ohio). 2014;32(6):1616-28.
3. Deng J, Wang DX, Liang AL, Tang J, Xiang DK. Effects of baicalin on alveolar fluid clearance and α-ENaC expression in rats with LPS-induced acute lung injury. Can J Physiol Pharmacol. 2016;95(2):122-8.
4. Nie H, Cui Y, Wu S, Ding Y, Li Y. 1,25-Dihydroxyvitamin D enhances alveolar fluid clearance by upregulating the expression of epithelial sodium channels. J Pharm Sci. 2016;105(1):333-8.
5. Ji HL, Zhao R, Komissarov AA, Chang Y, Liu Y, Matthay MA. Proteolytic regulation of epithelial sodium channels by urokinase plasminogen activator: cutting edge and cleavage sites. J Biol Chem. 2015;290(9):5241-55.
6. He J, Qi D, Tang XM, Deng W, Deng XY, Zhao Y, et al. Rosiglitazone promotes ENaC-mediated alveolar fluid clearance in acute lung injury through the PPARgamma/SGK1 signaling pathway. Cell Mol Biol Lett. 2019;24:35.

7. Kellenberger S, Schild L. International Union of Basic and Clinical Pharmacology. XCI. structure, function, and pharmacology of acid-sensing ion channels and the epithelial Na+ channel. Pharmacol Rev. 2015;67(1):1-35.
8. Walter J, Ware LB, Matthay MA. Mesenchymal stem cells: mechanisms of potential therapeutic benefit in ARDS and sepsis. Lancet Respir Med. 2014;2(12):1016-26.
9. Lee JW, Gupta N, Serikov V, Matthay MA. Potential application of mesenchymal stem cells in acute lung injury. Expert Opin Biol Ther. 2009;9(10):1259-70.
10. Ornellas DS, Marongutierrez T, Ornellas FM, Cruz FF, Oliveira GP, Lucas IH, et al. Early and late effects of bone marrow-derived mononuclear cell therapy on lung and distal organs in experimental sepsis. Respir Physiol Neurobiol. 2011;178(2):304-14.
11. Lee JS, Hong JM, Moon GJ, Lee PH, Ahn YH, Bang OY. A long-term follow-up study of intravenous autologous mesenchymal stem cell transplantation in patients with ischemic stroke. Stem Cells. 2010;28(6):1099-106.
12. Williams AR, Hare JM. Mesenchymal stem cells: biology, pathophysiology, translational findings, and therapeutic implications for cardiac disease. Circ Res. 2011;109(8):923-40.
13. Sakata N, Goto M, Yoshimatsu G, Egawa S, Unno M. Utility of co-transplanting mesenchymal stem cells in islet transplantation. World J Gastroenterol. 2011;17(47):5150-5.
14. Lee JW, Anna K, Mckenna DH, Yuanlin S, Jason A, Matthay MA. Therapeutic effects of human mesenchymal stem cells in ex vivo human lungs injured with live bacteria. Am J Respir Crit Care Med. 2013;187(7):751-60.
15. Qin K, Zhong X, Wang D. MicroRNA-7-5p regulates human alveolar epithelial sodium channels by targeting the mTORC2/SGK-1 signaling pathway. Exp Lung Res. 2016, 42(5):237-44.
16. Staszel T, Zapala B, Polus A, Sadakierska-Chudy A, Kiec-Wilk B, Stepien E, et al. Role of microRNAs in endothelial cell pathophysiology. Pol Arch Med Wewn. 2011;121(10):361-6.
17. Lee JW, Fang X, Krasnodembskaya A, Howard JP, Matthay MA. Concise review: Mesenchymal stem cells for acute lung injury: role of paracrine soluble factors. Stem cells. 2011;29(6):913-9.
18. Chen J, Hu C, Pan P. Extracellular vesicle microRNA transfer in lung diseases. Front Physiol. 2017;8:1028.
19. Shukla GC, Singh J, Barik S. MicroRNAs: processing, maturation, target recognition and regulatory functions. Mol Cell Pharmacol. 2011;3(3):83-92.
20. Leung AKL, Sharp PA. MicroRNA functions in stress responses. Mol Cell. 2010;40(2):205-15.
21. Guo H, Ingolia NT, Weissman JS, Bartel DP. Mammalian microRNAs predominantly act to decrease target mRNA levels. Nature. 2010;466(7308):835-40.
22. Sessa R, Hata A. Role of microRNAs in lung development and pulmonary diseases. Pulm Circ. 2013;3(2):315-28.
23. Hwang B, Liles WC, Waworuntu R, Mulligan MS. Pretreatment with bone marrow-derived mesenchymal stromal cell-conditioned media confers pulmonary ischemic tolerance. J Thorac Cardiovasc Surg. 2016;151(3):841-9.
24. Zhu J, Bai J, Wang S, Dong H. Down-regulation of long non-coding RNA SNHG14 protects against acute lung injury induced by lipopolysaccharide through microRNA-34c-3p-dependent inhibition of WISP1. Respir Res. 2019;20(1):233.
25. Nie HG, Chen L, Han DY, Li J, Song WF, Wei SP, et al. Regulation of epithelial sodium channels by cGMP/PKGII. J Physiol. 2009, 587(Pt 11):2663-76.
26. Ding Y, Cui Y, Zhou Z, Hou Y, Pang X, Nie H. Lipopolysaccharide inhibits alpha epithelial sodium channel expression via miR-124-5p in alveolar type 2 epithelial cells. BioMed Res Int. 2020;2020:8150780.
27. Alli AA, Bao HF, Liu BC, Yu L, Aldrugh S, Montgomery DS, et al. Calmodulin and CaMKII modulate ENaC activity by regulating the association of MARCKS and the cytoskeleton with the apical membrane. Am J Physiol Renal Physiol. 2015, 309(5):F456-63.
28. Montgomery DS, Yu L, Ghazi ZM, Thai TL, Al-Khalili O, Ma HP, et al. ENaC activity is regulated by calpain-2 proteolysis of MARCKS proteins. Am J Physiol Cell Physiol. 2017;313(1):C42-C53.
29. Sigmarsdottir T, McGarrity S, Rolfsson O, Yurkovich JT, Sigurjonsson OE. Current status and future prospects of genome-scale metabolic modeling to optimize the use of mesenchymal stem cells in regenerative medicine. Front Bioeng Biotechnol. 2020;8:239.

30. Tsiapalis D, O'Driscoll L. Mesenchymal stem cell derived extracellular vesicles for tissue engineering and regenerative medicine applications. Cells. 2020;9(4):991.
31. Chang J, Ding Y, Zhou Z, Nie HG, Ji HL. Transepithelial fluid and salt re-absorption regulated by cGK2 signals. Int J Mol Sci. 2018;19(3):881.
32. Bartel DP. MicroRNAs: target recognition and regulatory functions. Cell. 2009;136(2):215-33.
33. Flynt AS, Lai EC. Biological principles of microRNA-mediated regulation: shared themes amid diversity. Nat Rev Genet. 2008;9(11):831-42.
34. Zhou Y, Li P, Goodwin AJ, Cook JA, Halushka PV, Chang E, et al. Exosomes from endothelial progenitor cells improve outcomes of the lipopolysaccharide-induced acute lung injury. Crit Care.2019;23(1):44.
35. Alli AA, Bao HF, Alli AA, Aldrugh Y, Song JZ, Ma HP, et al. Phosphatidylinositol phosphate-dependent regulation of Xenopus ENaC by MARCKS protein. Am J Physiol Renal Physiol. 2012;303(6):F800-11.

Figure Legends:

Fig. 1 BMSCs enhances the cell viability in mouse AT2 and H441 cells. CCK-8 cell proliferation assay under the condition of normal medium (Control), serum-free medium (SD), co-culture with BMSCs (Co-culture), and BMSCs-CM administration in AT2 (**A**) and H441 (**B**) cells. $^{**}P < 0.01$, compared with SD group, n = 5 ~ 6.

Fig. 2 BMSCs-CM increases the protein and mRNA expression of γ-ENaC after LPS adminstration. (**A, C**) Representative blots of γ-ENaC protein in control (Control), LPS (10 μg/ml, 12 h, LPS), BMSCs-CM (24 h, CM), and BMSCs-CM plus LPS (LPS + CM) group of mouse AT2 and H441 cells, respectively. (**B, D**) Graphical representation of data obtained from western blots and quantified through gray analysis (γ-ENaC/β-actin). (E) Real-time PCR results of γ-ENaC mRNA expression in mouse AT2 cells. $^{**}P < 0.01$, compared with Control group. $^{\&\&}P < 0.01$, compared with LPS group. n = 5 ~ 7.

Fig. 3 The expression of miR-34c is decreased in LPS-treated mouse AT2 cells. (**A**) The result of real-time PCR assay showing miR-34c level in control AT2 cells (Control), LPS (10 μg/ml, 12 h, LPS), BMSCs-CM (24 h, CM), and BMSCs-CM plus LPS (LPS + CM) group of mouse AT2 cells. Relative level of miR-34c was calculated as miR-34c /U6 ratios. $^{**}P < 0.01$, compared with Control group. $^{\&\&}P < 0.01$, compared with LPS group. n = 6. (**B**) Transfection efficiency of miR-34c in mouse AT2 cells. Cells were transfected with control (NC), negative control (NC), miR-34c mimics (Mimic), inhibitor negative control (Inhibitor NC), or miR-34c inhibitor (Inhibitor), respectively. $^{**}P < 0.01$, compared with NC group. $^{\&\&\&}P < 0.001$, compared with Inhibitor NC group. n = 4.

Fig. 4 The levels of miR-34c and γ-ENaC are positively correlated in mouse AT2 cells. (**A**)

Representative blots of γ-ENaC protein in AT2 cells transfected with miR-34c negative control (NC), miR-34c mimics (Mimic), inhibitor negative control (Inhibitor NC), or miR-34c inhibitor (Inhibitor). (**B**) Graphical representation of data obtained from western blots and quantified through gray analysis (γ-ENaC/β-actin). $^{*}P < 0.05$, compared with NC group. $^{\&\&}P < 0.01$, compared with Inhibitor NC group. n = 3.

Fig. 5 MiR-34c increases amiloride-sensitive short-circuit current in H441 monolayers. (**A**) Representative short-circuit current (Isc) traces recorded in confluent H441 monolayers transfected with miR-34c negative control (NC), miR-34c mimics (miR-34) for 48 h. (**B**) Percentage of amiloride-sensitive Isc (ASI %) in NC and miR-34 group. ASI was defined as the difference between the total current and the amiloride-resistant current, and the negative control (NC) was set as 100%. $^{**}P < 0.01$, compared with NC group. n = 5.

Fig. 6 Dual luciferase assay for miR-34c binding with MARCKS in mouse AT2 cells. (**A**) The potential binding sites for miR-34c on the 3′-UTRs of MARCKS. (**B**) AT2 cells were co-transfected with negative control (NC) or miR-34c mimics (Mimic) together with pmirGLO- MARCKS (WT or MT) for 24 h. $^{**}P < 0.01$, compared with NC group. n = 5.

Fig. 7 Potential mechanisms for miR-34c involved in MSCs-CM regulation of LPS-induced ALI. MiR-34c can bind 3'-UTR of MARKS and increase γ-ENaC expression and function indirectly in alveolar epithelial cells, which may enhance AFC and relieve MSCs-CM regulated edematous ALI. MSC, mesenchymal stem cell; CM, conditioned medium; ENaC, epithelial sodium channel; AFC, alveolar fluid clearance; miRNAs, microRNAs; AT1, alveolar type 1 epithelial cells; AT2, alveolar type 2 epithelial cells; ALI, acute lung injury.

Figure 1

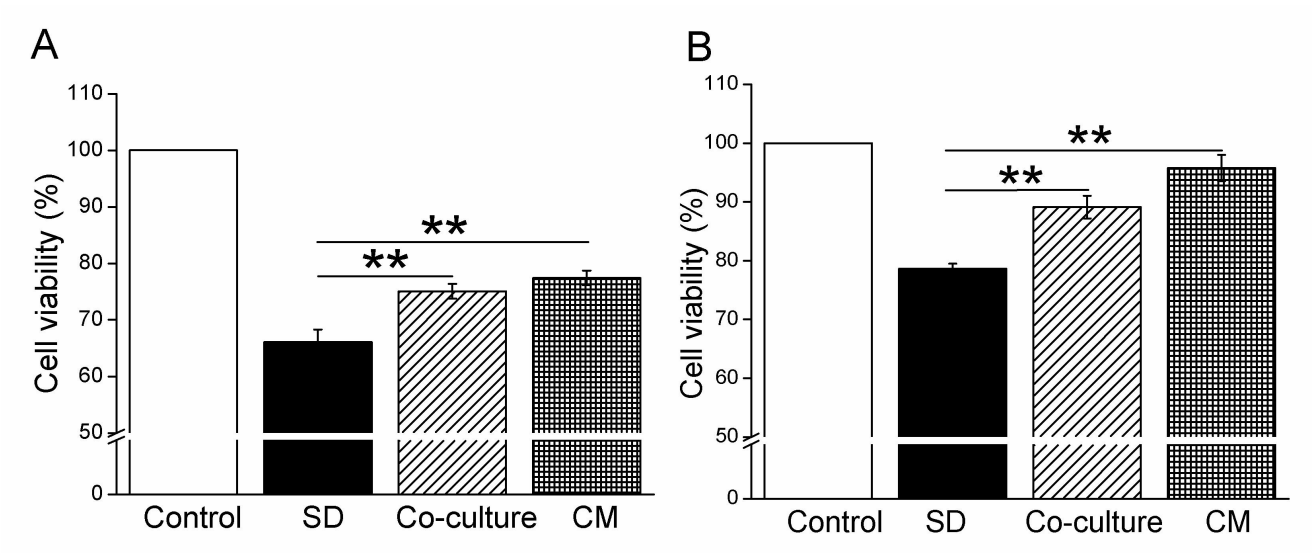
A
Cell viability (%)
110
100
90
80
70
60
50
0
**
**
Control
SD
Co-culture
CM
B
Cell viability (%)
110
100
90
80
70
60
50
0
**
**
Control
SD
Co-culture
CM

Figure 2

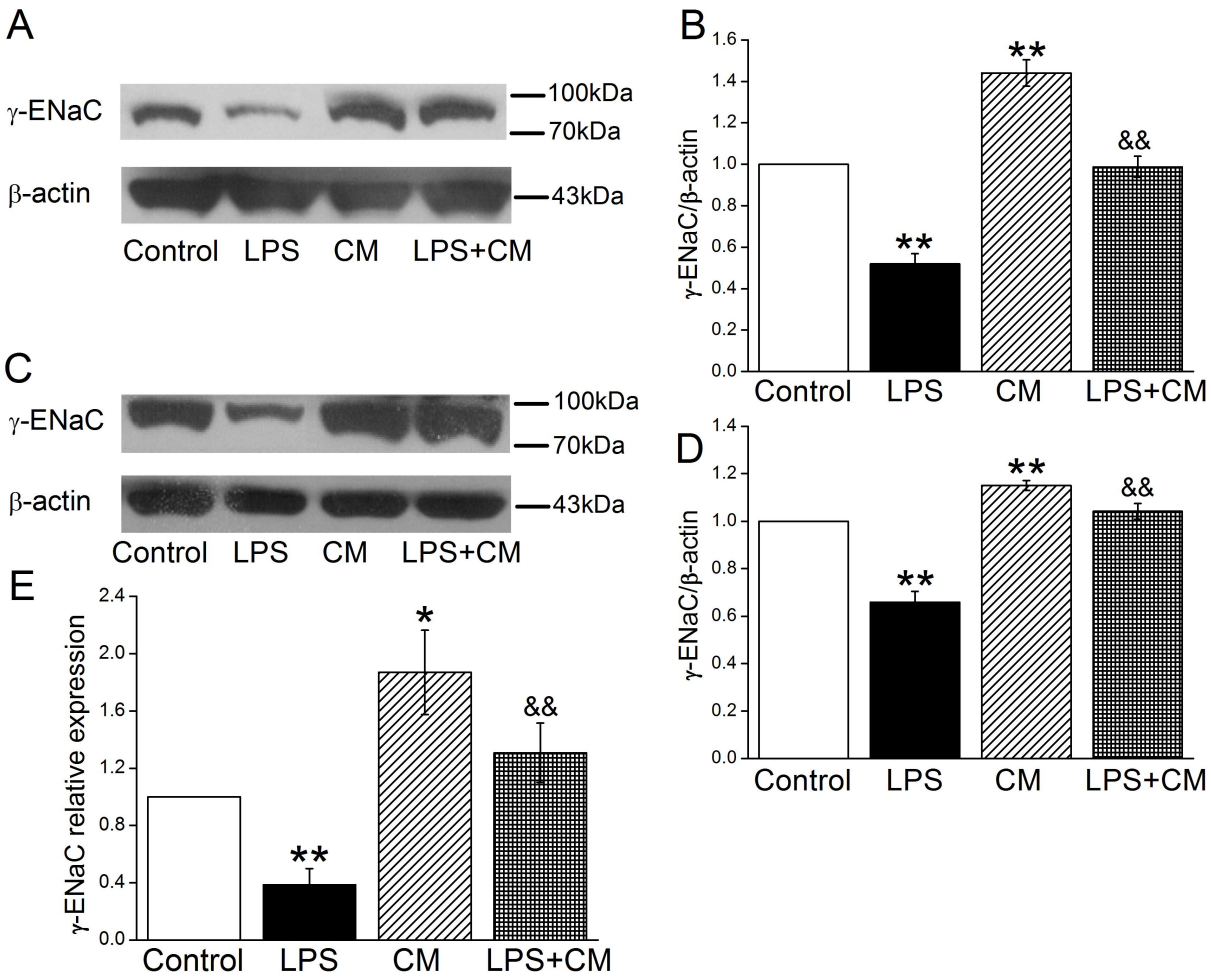
A
γ-ENaC
β-actin
100kDa
70kDa
43kDa
Control
LPS
CM
LPS+CM
B
γ-ENaC/β-actin
**
**
&&
C
γ-ENaC
β-actin
100kDa
70kDa
43kDa
Control
LPS
CM
LPS+CM
D
γ-ENaC/β-actin
**
**
&&
E
γ-ENaC relative expression
*
**
&&

Figure 3

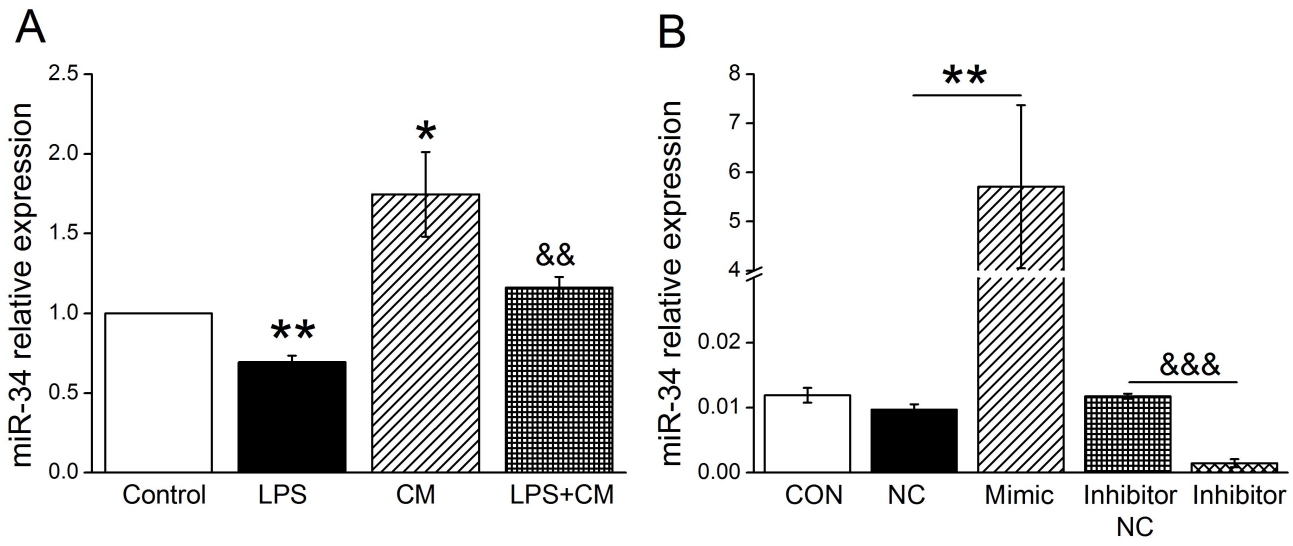
A
miR-34 relative expression
2.5
2.0
1.5
1.0
0.5
0.0
**
*
&&
Control
LPS
CM
LPS+CM
B
miR-34 relative expression
8
7
6
5
4
0.02
0.01
0.00
**
&&&
CON
NC
Mimic
Inhibitor NC
Inhibitor

Figure 4

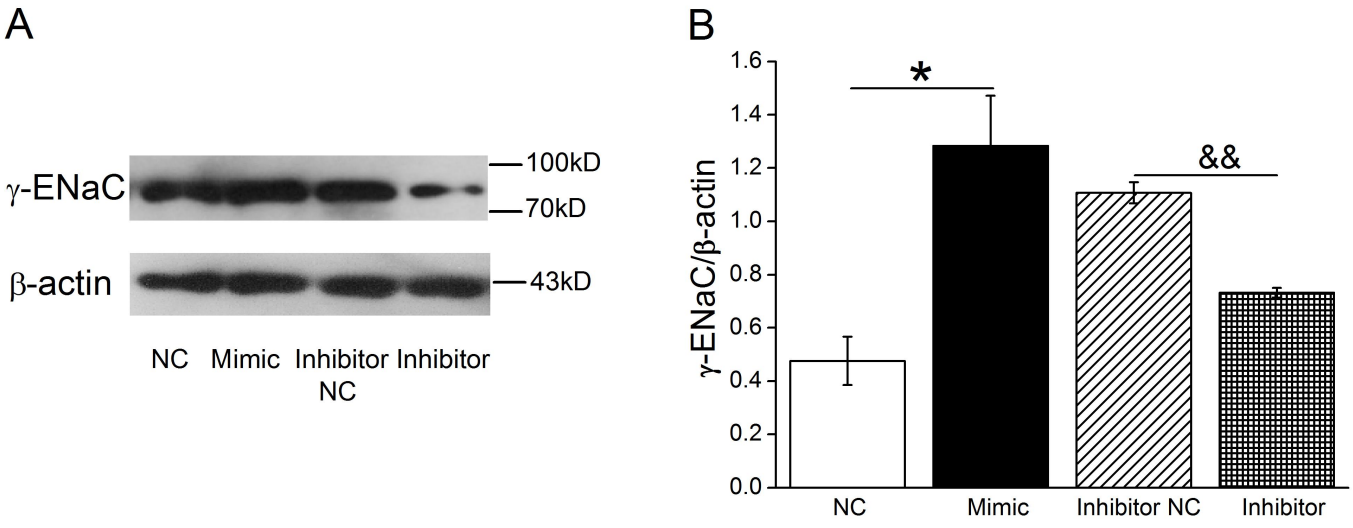
A
γ-ENaC
β-actin
100kD
70kD
43kD
NC
Mimic
Inhibitor NC
Inhibitor
B
γ-ENaC/β-actin
1.6
1.4
1.2
1.0
0.8
0.6
0.4
0.2
0.0
*
&&
NC
Mimic
Inhibitor NC
Inhibitor

Figure 5

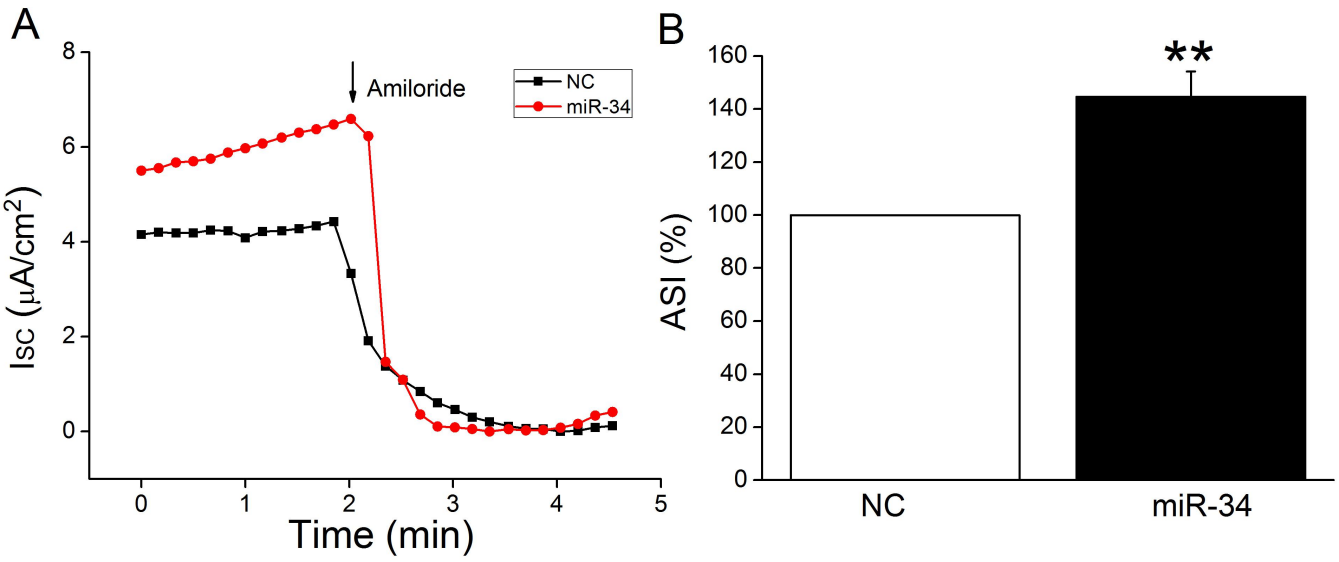

Figure 6

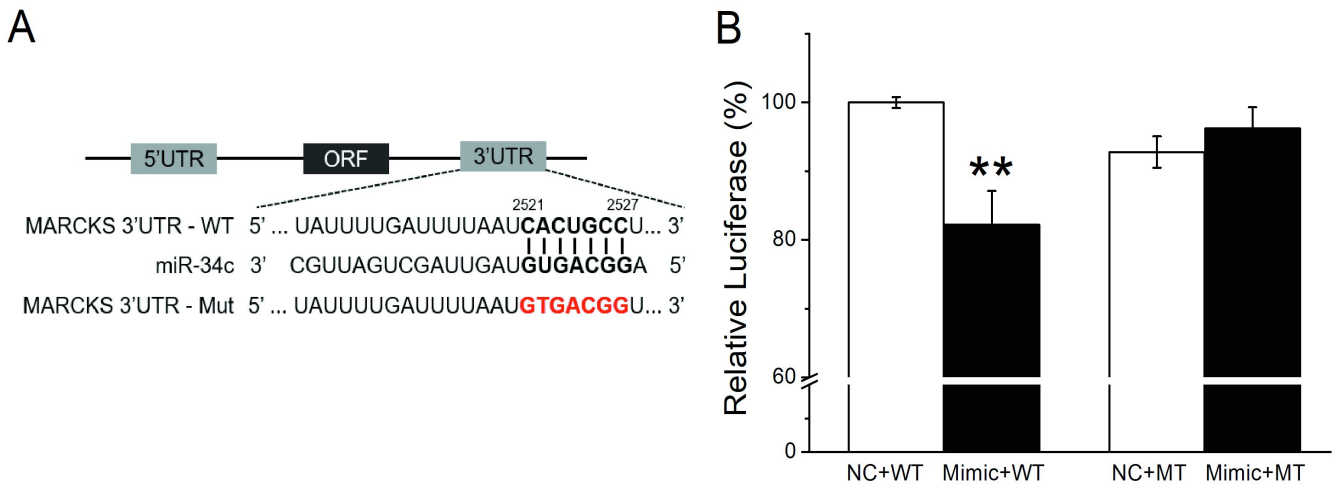
A
5'UTR
ORF
3'UTR
2521
2527
MARCKS 3'UTR - WT 5' ... UAUUUUGAUUUUAAUCACUGCCU... 3'
miR-34c 3' CGUUAGUCGAUUGAUGUGACGGA 5'
MARCKS 3'UTR - Mut 5' ... UAUUUUGAUUUUAAUGTGACGGU... 3'
B
Relative Luciferase (%)
100
80
60
0
**
NC+WT
Mimic+WT
NC+MT
Mimic+MT

Figure 7

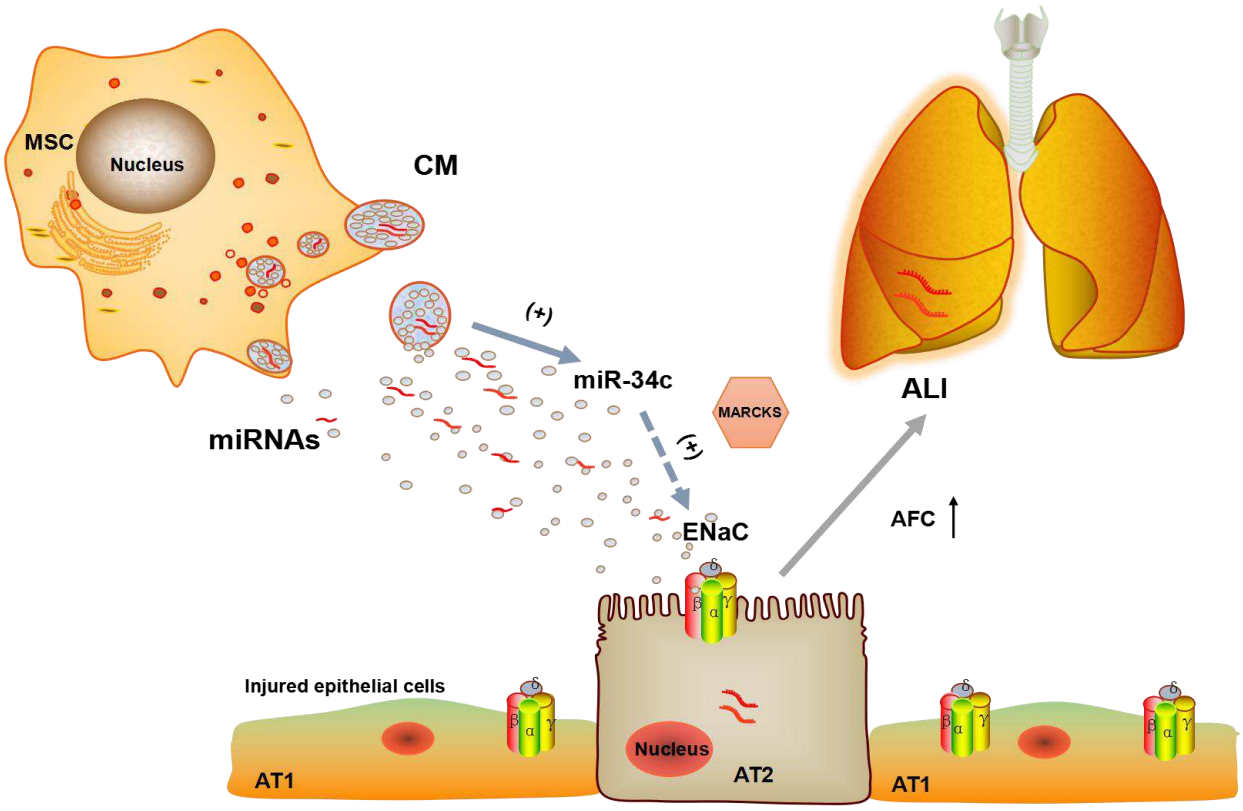
MSC
Nucleus
CM
miRNAs
(+)
miR-34c
MARCKS
(-)
ENaC
ALI
AFC
Injured epithelial cells
AT1
Nucleus
AT2
AT1

Supplementary information

Supplementary Fig. 1 Identification of BMSCs. Cells were incubated with antibodies of CD34 (A) and CD44 (B), respectively, and identified by flow cytometry.

Supplementary Fig. 2 Identification of AT2 cells. Immunofluorescence results of AT2 cells stained with DAPI (A), SP-C (**B**) or both (**C**), respectively. Magnification is 1:400.

Supplementary Figure 1

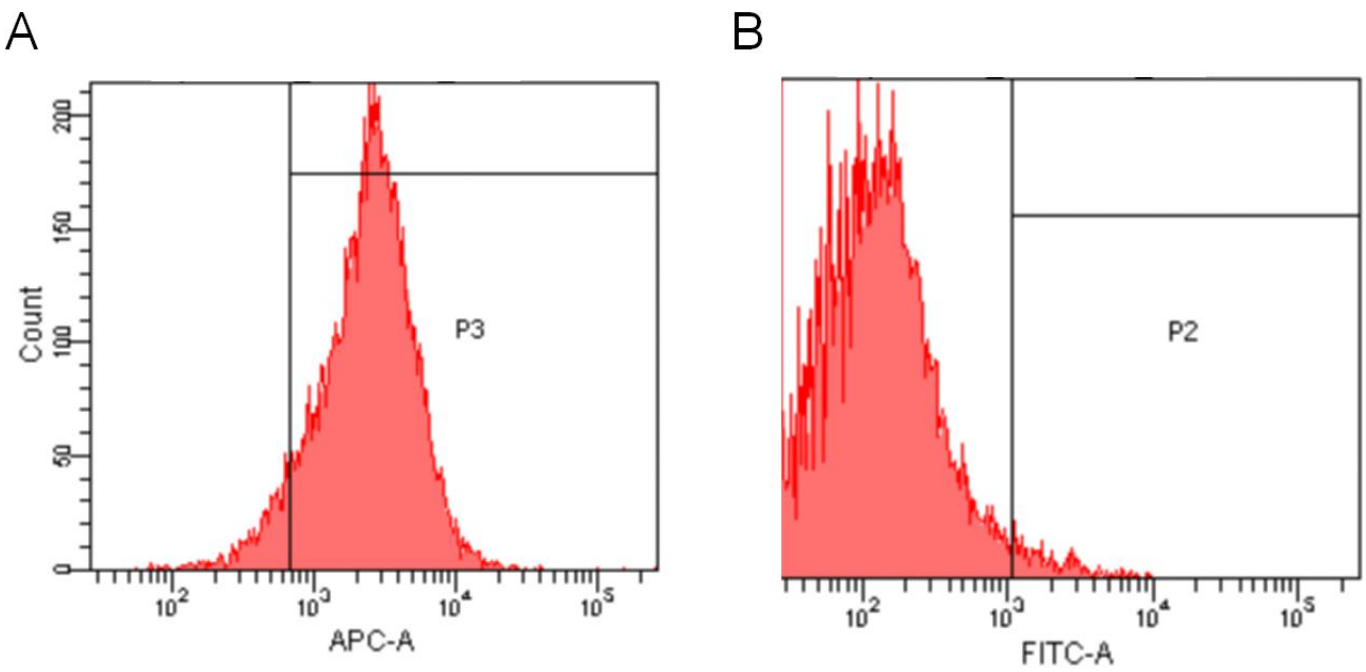

Supplementary Figure 2

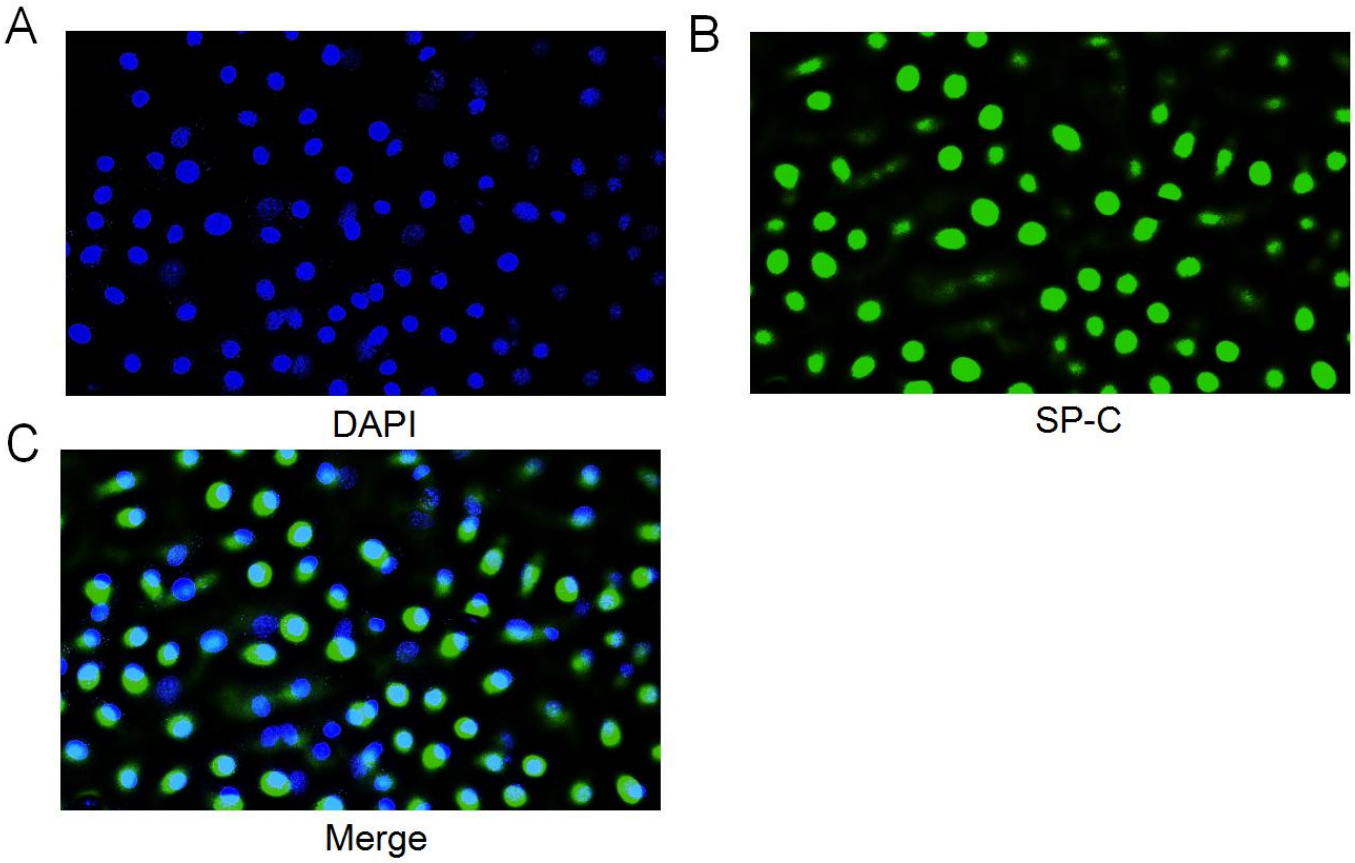

Figures

Figure 1

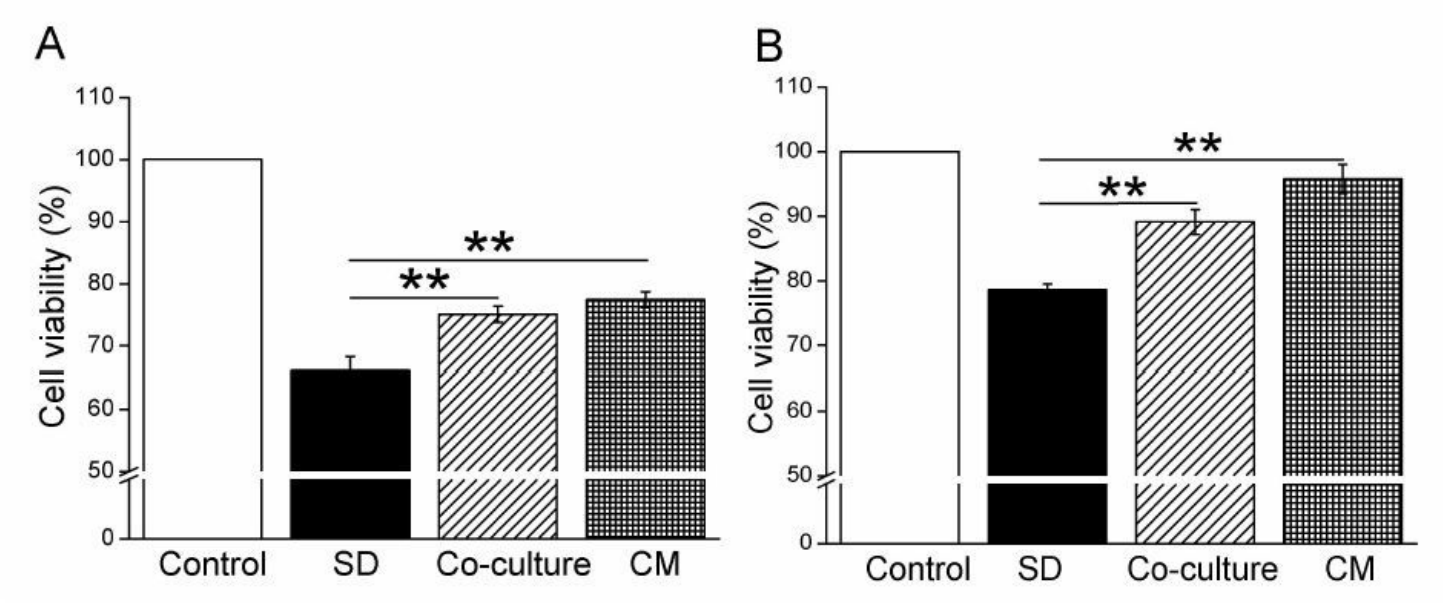

Figure 1

BMSCs enhances the cell viability in mouse AT2 and H441 cells. CCK-8 cell proliferation assay under the condition of normal medium (Control), serum-free medium (SD), co-culture with BMSCs (Co-culture), and BMSCs-CM administration in AT2 (A) and H441 (B) cells. **P < 0.01, compared with SD group, n = 5 ~ 6.

Figure 2

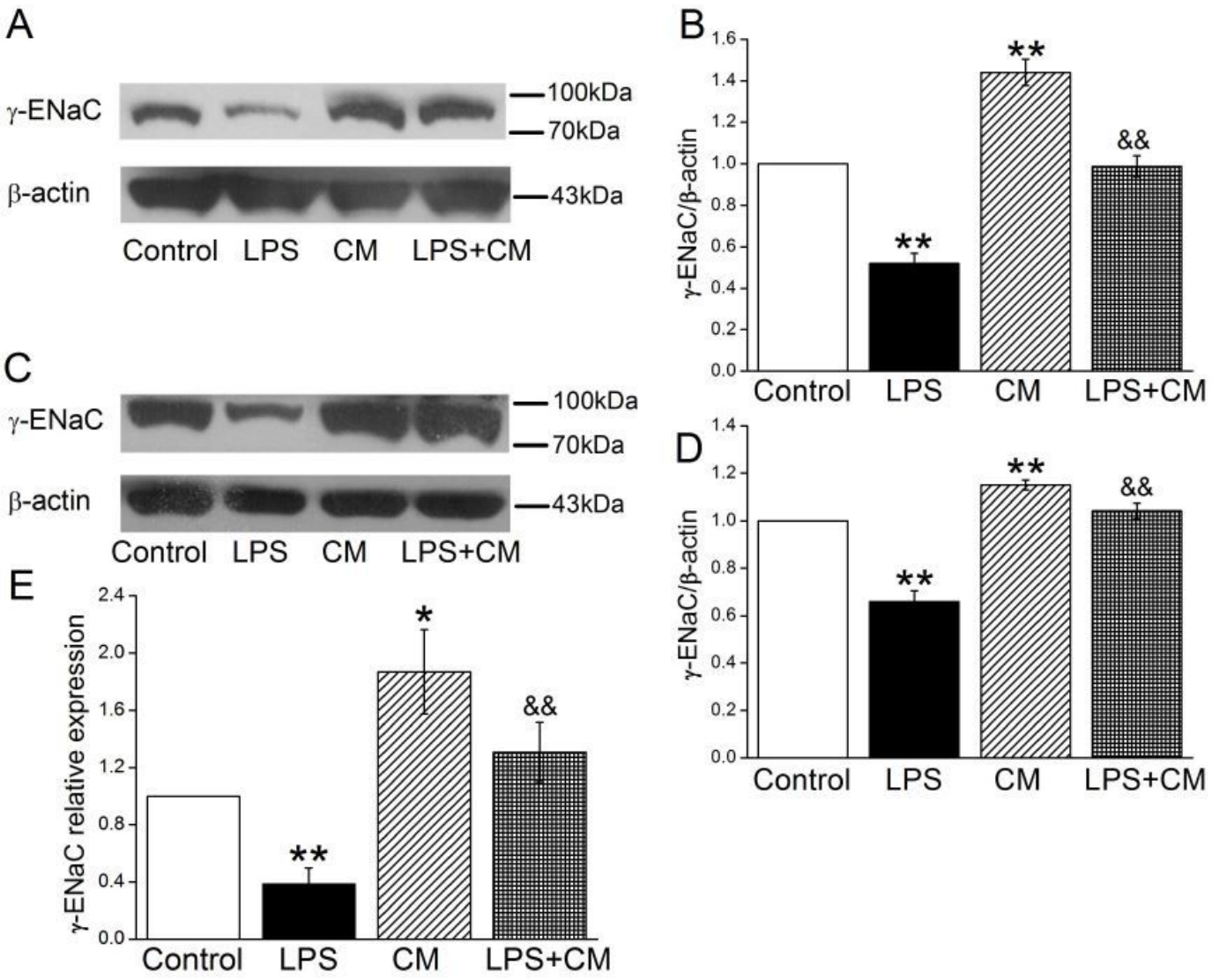

Figure 2

BMSCs-CM increases the protein and mRNA expression of γ-ENaC after LPS adminstration. (A, C) Representative blots of γ-ENaC protein in control (Control), LPS (10 μg/ml, 12 h, LPS), BMSCs-CM (24 h, CM), and BMSCs-CM plus LPS (LPS + CM) group of mouse AT2 and H441 cells, respectively. (B, D) Graphical representation of data obtained from western blots and quantified through gray analysis (γ-ENaC/β-actin). (E) Real-time PCR results of γ-ENaC mRNA expression in mouse AT2 cells. **P < 0.01, compared with Control group. &&P < 0.01, compared with LPS group. n = 5 ~ 7.

Figure 3

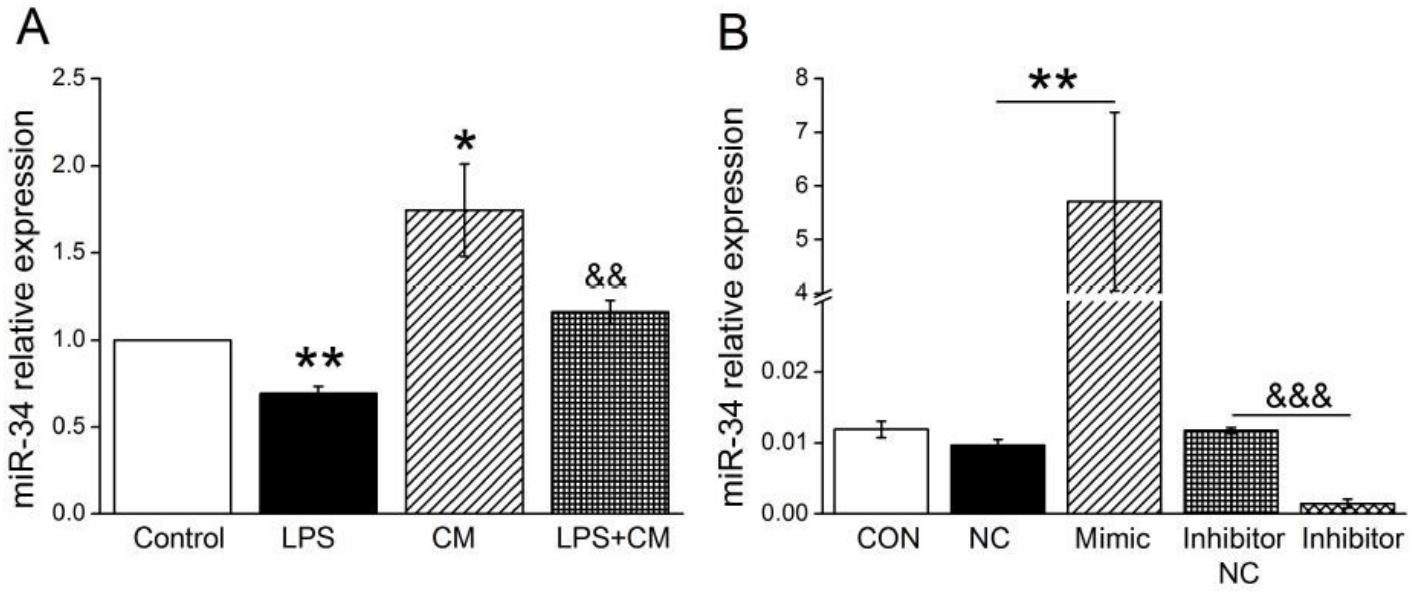

Figure 3

The expression of miR-34c is decreased in LPS-treated mouse AT2 cells. (A) The result of real-time PCR assay showing miR-34c level in control AT2 cells (Control), LPS (10 μg/ml, 12 h, LPS), BMSCs-CM (24 h, CM), and BMSCs-CM plus LPS (LPS + CM) group of mouse AT2 cells. Relative level of miR-34c was calculated as miR-34c /U6 ratios. **P < 0.01, compared with Control group. &&P < 0.01, compared with LPS group. n = 6. (B) Transfection efficiency of miR-34c in mouse AT2 cells. Cells were transfected with control (NC), negative control (NC), miR-34c mimics (Mimic), inhibitor negative control (Inhibitor NC), or miR-34c inhibitor (Inhibitor), respectively. **P < 0.01, compared with NC group. &&&P < 0.001, compared with Inhibitor NC group. n = 4.

Figure 4

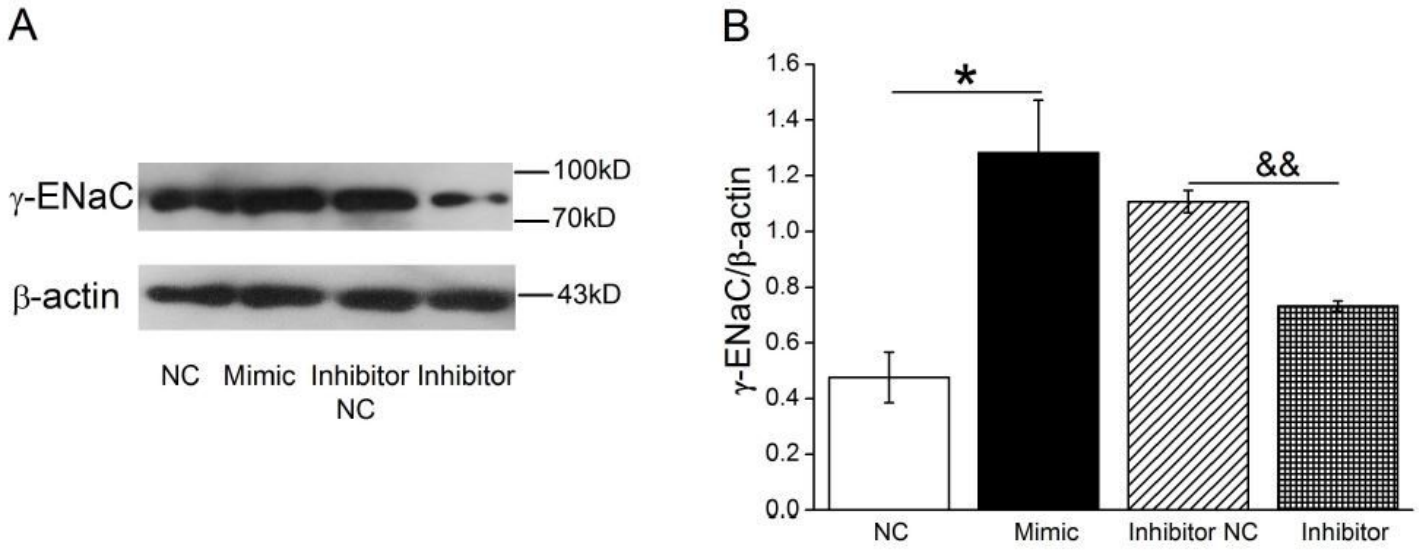

Figure 4

The levels of miR-34c and γ-ENaC are positively correlated in mouse AT2 cells. (A) Representative blots of γ-ENaC protein in AT2 cells transfected with miR-34c negative control (NC), miR-34c mimics (Mimic), inhibitor negative control (Inhibitor NC), or miR-34c inhibitor (Inhibitor). (B) Graphical representation of data obtained from western blots and quantified through gray analysis (γ-ENaC/β-actin). *P < 0.05, compared with NC group. &&P < 0.01, compared with Inhibitor NC group. n = 3.

Figure 5

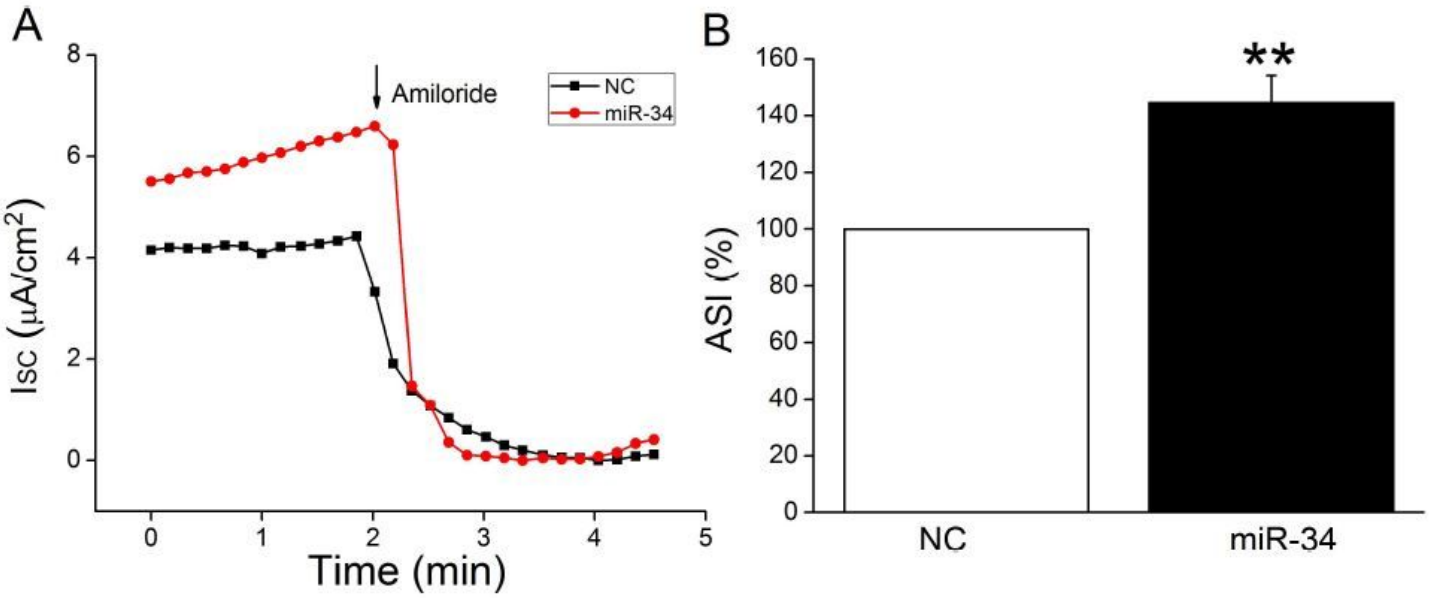

Figure 5

MiR-34c increases amiloride-sensitive short-circuit current in H441 monolayers. (A) Representative short-circuit current (Isc) traces recorded in confluent H441 monolayers transfected with miR-34c negative control (NC), miR-34c mimics (miR-34) for 48 h. (B) Percentage of amiloride-sensitive Isc (ASI %) in NC and miR-34 group. ASI was defined as the difference between the total current and the amiloride-resistant current, and the negative control (NC) was set as 100%. **P < 0.01, compared with NC group. n = 5.

Figure 6

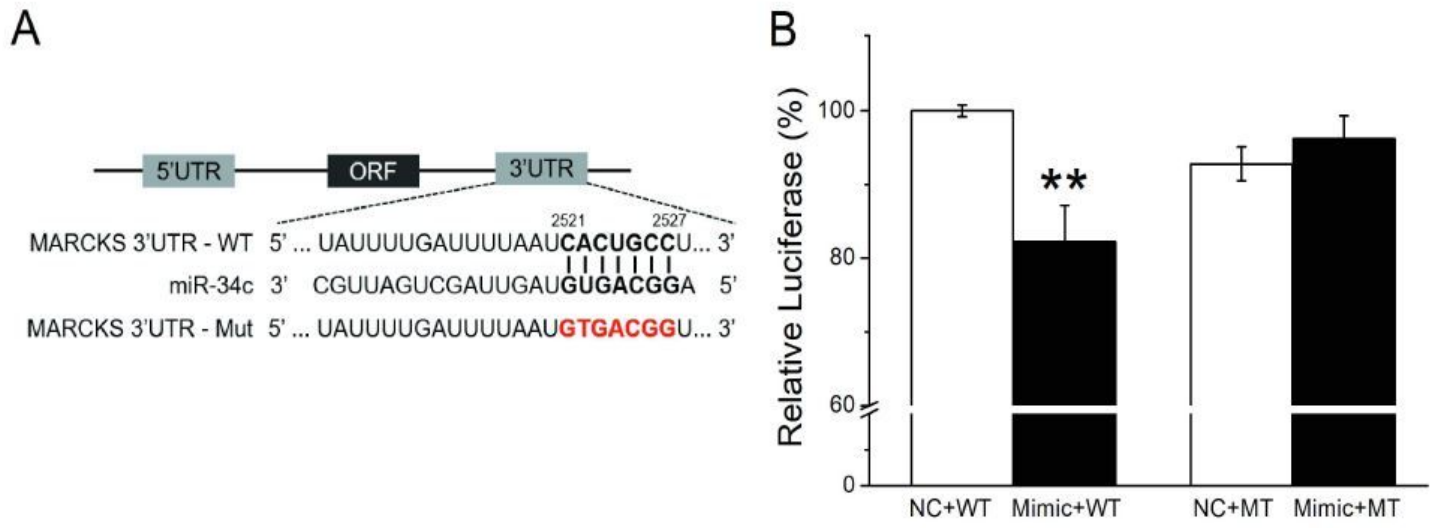

Figure 6

Dual luciferase assay for miR-34c binding with MARCKS in mouse AT2 cells. (A) The potential binding sites for miR-34c on the 3'-UTRs of MARCKS. (B) AT2 cells were co-transfected with negative control (NC) or miR-34c mimics (Mimic) together with pmirGLO- MARCKS (WT or MT) for 24 h. **P < 0.01, compared with NC group. n = 5.

Figure 7

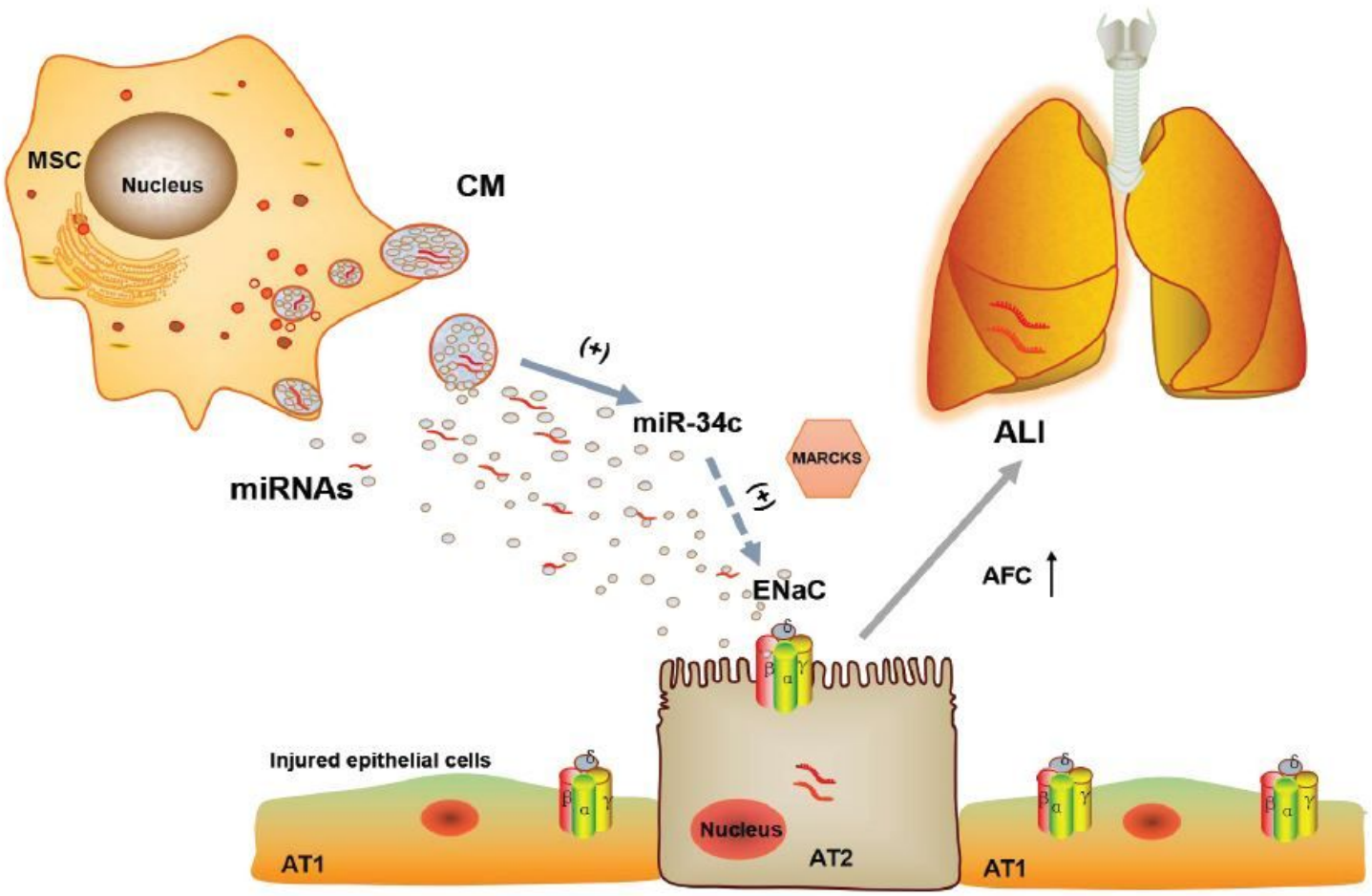

Figure 7

Potential mechanisms for miR-34c involved in MSCs-CM regulation of LPS-induced ALI. MiR-34c can bind 3'-UTR of MARKS and increase γ-ENaC expression and function indirectly in alveolar epithelial cells, which may enhance AFC and relieve MSCs-CM regulated edematous ALI. MSC, mesenchymal stem cell; CM, conditioned medium; ENaC, epithelial sodium channel; AFC, alveolar fluid clearance; miRNAs, microRNAs; AT1, alveolar type 1 epithelial cells; AT2, alveolar type 2 epithelial cells; ALI, acute lung injury.